Hopping Domain Wall Induced by Paired Adatoms on an Atomic Wire: Si(111)-(5 × 2)-Au

Pil-Gyu Kang, Hojin Jeong, and Han Woong Yeom*

Institute of Physics and Applied Physics and Center for Atomic Wires and Layers, Yonsei University, Seoul 120-749, Korea

(Received 15 October 2007; published 11 April 2008)

We observed an inhomogeneous fluctuation along one-dimensional atomic wires self-assembled on a Si(111) surface using scanning tunneling microscopy. The fluctuation exhibits dynamic behavior at room temperature and is observed only in a specific geometric condition; the spacing between two neighboring adatom defects is discommensurate with the wire lattice. Upon cooling, the dynamic fluctuation freezes to show the existence of an atomic-scale dislocation or domain wall induced by such ''unfavorably'' paired adatoms. The microscopic characteristics of the dynamic fluctuation are explained in terms of a hopping solitonic domain wall, and a local potential for this motion imposed by the adatoms is quantified.

DOI: 10.1103/PhysRevLett.100.146103 PACS numbers: 68.35.Dv, 68.37.Ef, 68.43.Fg, 68.65.−k

One-dimensional (1D) materials systems have been the subject of extensive studies because of a variety of exotic physical phenomena due to enhanced many-body interactions and fluctuations and potential applications in nano and molecular devices [1]. Recently, self-organized 1D systems formed by Au adsorption on Si surfaces, such as Si(557)-Au [2–4], Si(553)-Au [3,5], and Si(111)-(5 × 2)-Au [6–9], have provided new playgrounds for 1D physics research due to their well-ordered atomic wire structures with well-defined 1D metallic bands. These atomic wires commonly inherit various impurities, such as vacancies and adsorbates. It is general wisdom that, in a 1D system, even the weak scattering by low-density impurities can drastically change the electronic property as manifested in Anderson localization [10]. In Au/Si atomic wire systems, the strong coupling of the impurities with charge-density wave was already suggested [11,12]. However, much is left unknown for possible effects of impurities, especially when it comes down to the atomic scale for individual or coupled [13] impurities.

Among the 1D metallic wire systems on Si surfaces, the Si(111)-(5 × 2)-Au system has been known to feature unique double Au rows in a unit wire [see Fig. 1(d) for the schematics of a structure model] [6–8]. Some of the Si atoms substituted by Au become adatom impurities distributed randomly along the wires [the bright protrusions in the STM image of Fig. 1(a)] [9,14]. It has been shown that this adatom impurity plays an active role in determining the electronic property of the atomic wire [15–17]. Moreover, the density of adatoms is controllable atom by atom with scanning tunneling microscope [18] or globally by Si deposition [17]. These previous works make the Si(111)-(5 × 2)-Au system very attractive for a systematic study on the interactions of active impurities with atomic wires.

In this Letter, we disclose a new type of the interaction between the impurity and the atomic wire: the dynamic fluctuation (DF) induced by the lattice frustration given by a pair of impurities. The ''discommensurately'' paired adatoms along the wire induce an atomic-scale lattice dislocation or domain wall, which hops between the paired adatoms to produce a characteristic DF at room temperature (RT). The potential landscape for the motion of this 1D domain wall is deduced.

The experiment was carried out using a commercial variable-temperature STM (Omicron, Germany). The Si(111)-(5 × 2)-Au surface with a well-ordered atomic wire array was prepared by deposition of 0.4 monolayer Au onto the clean Si(111)-(7 × 7) surface at 930 K [9,19]. The Si adatom density [9] was optimized to about 0.019 monolayer by thermal treatment [17]. Scanning tunneling microscope measurements were performed at RT and 25 K.

Figure 1(a) shows a typical STM image of the Si(111)-(5 × 2)-Au surface [(5 × 2)-Au hereafter]. The bare, undoped wire is characterized by a 5 × 2 unit cell (the rectangle) with a $5a_0$ spacing between the neighboring wires and a $2a_0$-period structure along the wire

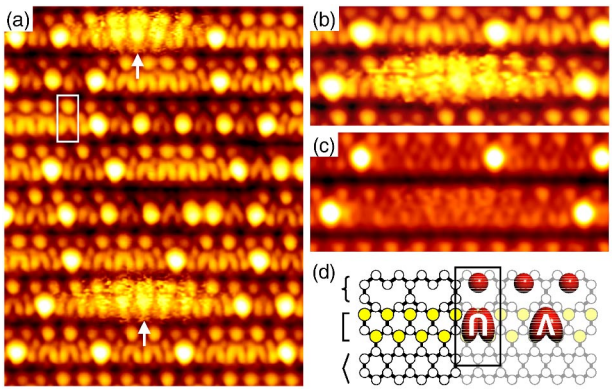

FIG. 1 (color online). (a) STM image (11×14 nm^2) of Si(111)-(5 × 2)-Au at RT and its close-ups in (b) empty and (c) filled states. Bias voltages are (a), (b) +1.0 and (c) −1.0 V and the tunneling current is 50 pA. (d) The schematics of one structure model [15], where large (yellow) and small (open) circles represent Au and Si atoms, respectively. Schematics of the characteristic features of the empty-state STM images are overlapped in the right. The 5 × 2 unit cell is depicted by boxes in (a) and (d).

[$a_0 = 3.84$ Å is the lattice constant of Si(111)]. In the empty-state STM image, the unit cell is composed of a ball- (''head'') and a $\bigcap$-shaped protrusion (''leg'') [7,20]. A recent structure model [Fig. 1(d)] consists mainly of a Si honeycomb chain and a double Au-Si chain (marked by ⟨ and [in the figure, respectively). This unit is connected with the neighboring one by bridging Si atoms ({ in the figure), which make the $2a_0$ periodicity [15]. On the other hand, a Si impurity, the prominently bright protrusion in STM [14], adsorbs stably in the center of the double Au-Si chain [15]. This structure model itself is not conclusive yet with the incomplete matching with the STM images [20] and with more recent alternatives [21]. The following discussion, however, does not depend on the detailed atomic structure of the wires. The adjacent Si adatoms distort the bare wire lattice to some extent; the $\bigcap$-shaped leg under a head converts into a Λ shaped one between two heads [20].

In addition to those well-established atomic features of 5×2-Au, we found a strong inhomogeneous contrast indicated by arrows in Fig. 1(a). The inhomogeneity is conspicuous in the empty state as characteristically composed of several noisy oval features with an interval of roughly $2a_0$ [Fig. 1(b)]. In the filled state [Fig. 1(c)], the contrast is very weak and fussy, but the normal $2a_0$ structure is observed to be partly destroyed.

We noticed that this inhomogeneous contrast is not static but fluctuating from the flickering stripe features along the scanning direction, which is typical for a fast-moving object under the tunneling tip [22]. In order to investigate the dynamic behavior, we followed the time dependence of the STM image. Figure 2(a) shows a part of sequential line profiles (with an interval of two seconds) of the fluctuation along the center of the wire in the empty-state image (the dashed line). In between two adatoms (arrowheads), there are small but discernible corrugations with a roughly $2a_0$ periodicity. Among them, a noticeably stronger peak (arrow) moves randomly. In particular, this peak is observed mainly at $5.5a_0$, $7.5a_0$, $9.5a_0$, $11.5a_0$, and $13.5a_0$ and less frequently at $3.5a_0$ and $15.5a_0$ away from the left adatom. These ''odd'' peak positions are not matched with any corrugation of normal 5×2-Au. In the filled-state image [Fig. 2(b)], similar sequential line profiles were taken along the row of head units. A similar time-dependent change is observed in the central region (gray part) involving a $1a_0$ or $3a_0$ spacing, which is not compatible with the normal 5×2 structure either. However, the lattice is obviously static within $3a_0$ from the adatoms in both empty and filled states. This result verifies that the inhomogeneity is a dynamic fluctuation and cannot be explained by the pristine wire structure.

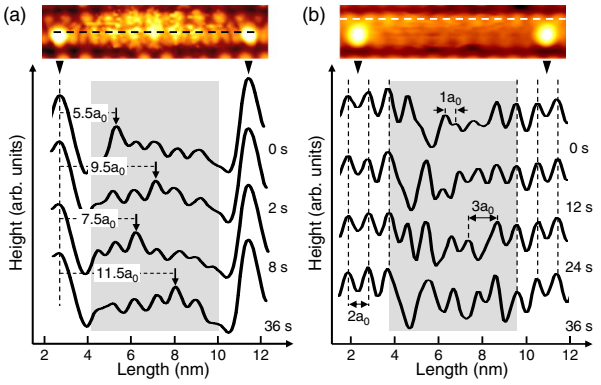

FIG. 2 (color online). STM images (top) in (a) empty and (b) filled states and sequential line profiles (lower 4 curves) along dashed lines of the images, respectively. Bias voltages are (a) +1.0 V and (c) −1.0 V and the tunneling current is 50 pA. Within the gray area, over $3a_0$ from adatoms, the line profile is time dependent.

However, as noticed easily in Fig. 1(a), only very few adatom pairs have the fluctuation. In order to understand the relationship between the adatoms and the fluctuation, the length distribution of a bare wire segment defined by two neighboring adatoms is measured as shown in Fig. 3. This distribution is very consistent with the previous measurement [9] with two characteristics: (i) the length is seldom an odd multiple of a_0 (''odd-length'' hereafter), indicating that this case is energetically unfavorable due to the $2a_0$-period lattice of the bare wire [9], and (ii) the distribution among even multiples of a_0 (''even-length'' hereafter) indicates a random occupation (a Poisson distribution) except for the strong adatom-adatom repulsion at $2a_0$.

The length of a bare wire segment defined by an adatom pair governs strictly the occurrence of the DF. Without any

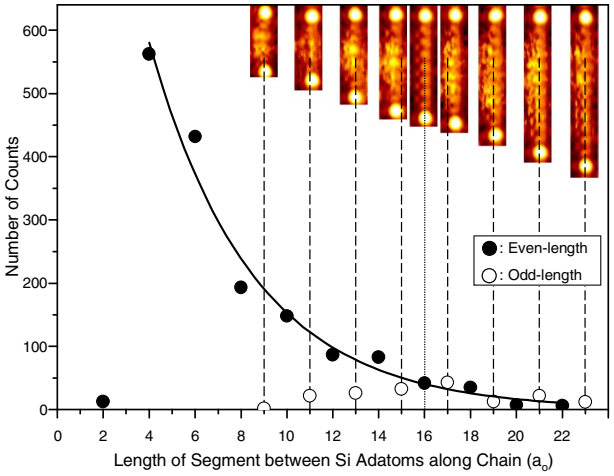

FIG. 3 (color online). Length distribution of the bare wire segments between two neighboring adatoms obtained from STM images (total 1836 Si adatoms are sampled). The distribution of the segment with a length of an even multiple of a_0 (solid circles) is fitted by a simple exponential function (solid line) of Poisson behavior except for a rarely observed one of $2a_0$ length. The segments with a length of an odd multiple of a_0 feature the DF without an exception, as shown in STM images (+ 1.0 V, 50 pA).

exception over far more than a thousand segments sampled, the DF is found only in odd-length segments as exemplified in the STM images within Fig. 3. In sharp contrast, no even-length segment exhibits the DF; only one example of $16a_0$ is shown in the figure. Going back to Fig. 1(a), the segments with DF have $15a_0$ and $19a_0$ in length, and all other segments have even lengths. This indicates that the DF is induced by the geometrical condition, the odd length or the deviation from the normal $2a_0$ periodicity of a wire, imposed by paired adatoms.

Then the sample was cooled down to possibly freeze the dynamic motion. Figure 4(a) shows an STM image of $5 \times$ 2-Au at 25 K. The DF is not observed at all for very wide areas and for different samples. Instead, a new atomic-scale feature is observed with a bright butterfly-shape contrast (arrows) for every odd-length segment. In the empty-state image of Fig. 4(b), this contrast is composed of two very close head units with an a_0 separation, two distorted Λ units, and a bright central protrusion [see Fig. 4(d) for the schematics]. In the filled-state image of Fig. 4(c), mainly a dark central trench is observed. Since this feature is never found in an even-length segment and its position within an odd-length segment is quite random, it is straightforward to assign them as the frozen state of the DF of RT. In addition, the overall brightness of this feature in the whole bias range is consistent with that of the RT DF.

Based on these results, one can understand the atomistic origin of the DF. Given the $2a_0$ periodicity of $5 \times$ 2-Au, an odd-length segment has no choice but to make a domain wall between two out-of-phase $\times 2$ lattices inside by introducing one a_0 unit. This domain wall or dislocation appears as two heads with an a_0 separation and the strong center protrusion in the empty-state image [Figs. 4(b) and 4(d)]. The strong distortion of the nearest-neighbor sites is shown by the distorted Λ units in both sides. That is, the domain wall is a truly atomic-scale object as being fairly well localized within a length of $3a_0$-$5a_0$.

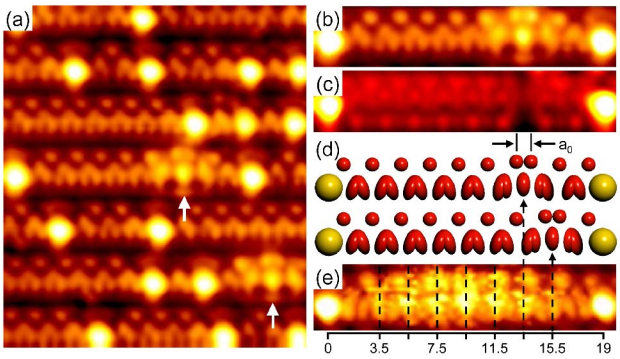

FIG. 4 (color online). (a) STM image (9.5×10.5 nm^2) of Si(111)-(5×2)-Au at 25 K. The dual-bias scanned STM images [empty-state in (b) and filled-state in (c)] for an odd-length ($19a_0$) segment include a new atomic feature. (d) Schematics of the empty-state STM image with two possible positions of the domain wall (the center of the strongly bright contrast in empty-state and the dark trench in filled-state), $13.5a_0$ and $15.5a_0$ from the left adatom. Large (yellow) circles represent Si adatoms. (e) An empty-state STM image for a $19a_0$ segment at RT. Bias voltages are (a),(b),(e) $+1.0$ V and (c) -1.0 V and the tunneling current is 50 pA.

Since the DF is confined beyond $3a_0$ from adatoms as shown by the gray areas in Fig. 2, the possible sites of such a domain wall can be easily deduced. For example, in case of a segment with a $19a_0$ length, there are seven possible sites with regular intervals of $2a_0$: $3.5a_0$, $5.5a_0$, $7.5a_0$, $9.5a_0$, $11.5a_0$, $13.5a_0$, and $15.5a_0$ from the left adatom. Two of these sites are shown schematically in Fig. 4(d), $13.5a_0$, and $15.5a_0$. One can easily see that the $15.5a_0$ site (or $3.5a_0$ for the opposite side) is the closest possible site to the end adatom due to the lateral size of the domain wall itself [Fig. 4(d)]. These correspond exactly to the positions of the bright ovals of the RT fluctuation in empty states as shown in Fig. 4(e). As the length of the odd-length segment increases, the possible sites of the dislocation increase systematically, which is fully consistent with the increase of the number of the oval features as shown in the STM images of Fig. 3. This indicates that the oval features at RT represent possible sites of the domain wall. In fact, the array of the oval features is a time-averaged image of the randomly moving peak (the central protrusion of the domain wall) in the snap shots of Fig. 2(a). That is, we found the possible hopping sites of a domain wall on an atomic wire and captured its hopping motion in a snapshot fashion with STM.

Furthermore, we directly measured the frequency for a moving domain wall to visit each site. Basically, we very slowly scanned the STM tip along the center of a fluctuating segment in empty state and probed the fast height fluctuation in real time at each site. Figure 5(a) shows the time dependence of the height measured on each site of Fig. 4(e). The height fluctuates between two well-defined positions, which should correspond to the domain wall and the bare site. Then the frequency of the fluctuation at each site was measured, which is of an order of several Hz. The frequency depends on the sites systematically, larger at the center ($0a_0$) than at both sides (for example $-6a_0$). That is, the domain wall is more favored near the center of the segment. This is also reflected in the envelope (apparent height) of the time-averaged image of the DF as shown in Fig. 5(c) (the gray line).

The quantitative measurement of the frequency in atomic scale allows us to determine the relative energy difference between the sites of the domain wall; the potential energy can be roughly described as shown in Fig. 5(b). If we assume a widely used attempt frequency prefactor (Γ_0) of 10^{13} Hz, the activation energy E_a for a domain wall hopping is estimated to be 0.5–0.7 eV, which is greatly larger than the thermal energy at RT. Therefore we can consider only the single jump for the domain wall hopping. At equilibrium, the motion is balanced as the rate

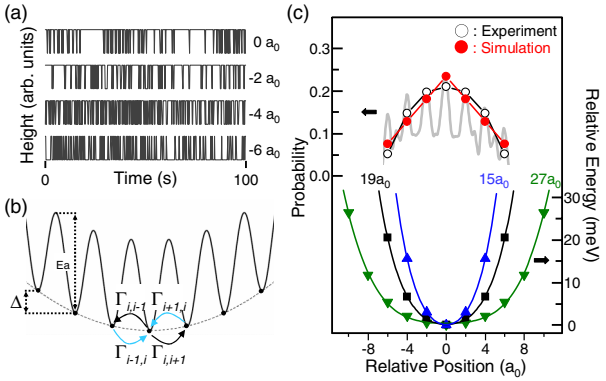

FIG. 5 (color online). (a) Time-dependent height at the centers of a few oval protrusions along dashed lines of Fig. 4(e) at RT after filtering small amplitude noise out. (b) The simple potential energy assumed for the domain wall hopping motion with the hopping events at a specific site. (c) (Upper) The occupation probability (both experiment and simulation) and (lower) the relative energy deduced as a function of distance from the center of the segments. The experimental data were taken for three different segments with lengths of 15, 19, and $27a_0$, but only one ($19a_0$) is shown. The gray solid line represents the envelope (apparent height) along the center of the DF in the time-averaged STM image.

equation, $dP_i/dt = P_{i-1}\Gamma_{i-1,i} + P_{i+1}\Gamma_{i+1,i} - P_i(\Gamma_{i,i-1} + \Gamma_{i,i+1}) = 0$, where P_i is the occupation probability for the domain wall at the site i, and $\Gamma_{i,i\pm1}$ is the transition rate from i to the neighboring sites [Fig. 5(b)]. In order to solve these rate equations, we make simple but reasonable first approximations: (i) the difference in E_a at each site is decided only by the relative energy difference between two sites Δ [Fig. 5(b)], (ii) Δ is a smoothly varying function of the position of the domain wall, and (iii) Γ_0 is constant over the sites. Then the relative energy was obtained by matching the calculated occupation probability to the measured ones from three different segments of 15, 19, and $27a_0$ [Fig. 5(c)]. A reasonably good match was obtained for the energy function inversely proportional to the distance from the adatom as shown in the figure. This fully justifies the repulsive interaction between the moving domain wall and adatoms. This interaction energy is of an order of 30 meV at maximum, which is naturally attributed to the lattice strain imposed by the adatoms at both ends. This energy is very small compared to the activation energy itself, making the motion of the domain wall close to random walks.

A moving domain wall in 1D is generally a solitonic object. In many case, a 1D domain wall is described by the Frenkel-Kontorova model, which considers the equilibrium state of a linear chain of atoms coupled by (rather weak) springs in a sinusoidal potential [23]. However, in order to check the validity of this model in the present case, a detailed structural modeling of the domain wall is necessary to independently determine the potential parameters. This is not possible in the present case since the atomic structure of the present wires is not clear yet [21]. In any case, the unique feature of the present system is that a 1D domain wall is confined and its hopping motion is clearly revealed in atomic scale. Moreover, since it is possible to manipulate single adatoms by STM [18], the domain wall could be generated one by one and its motion could eventually be manipulated.

This work was supported by MOST through Center for Atomic Wires and Layers of the CRi program.

*yeom@yonsei.ac.kr

[1] George Grüner, *Density Waves in Solids* (Addison-Wesley, Reading, MA, 1994).
[2] R. Losio *et al.*, Phys. Rev. Lett. **86**, 4632 (2001).
[3] J. N. Crain *et al.*, Phys. Rev. Lett. **90**, 176805 (2003).
[4] J. R. Ahn, H. W. Yeom, H. S. Yoon, and I. W. Lyo, Phys. Rev. Lett. **91**, 196403 (2003).
[5] J. R. Ahn, P. G. Kang, K. D. Ryang, and H. W. Yeom, Phys. Rev. Lett. **95**, 196402 (2005).
[6] S. M. Durbin, L. E. Berman, B. W. Batterman, and J. M. Blakely, Phys. Rev. B **33**, 4402 (1986).
[7] A. A. Baski, J. Nogami, and C. F. Quate, Phys. Rev. B **41**, 10 247 (1990).
[8] L. D. Marks and R. Plass, Phys. Rev. Lett. **75**, 2172 (1995).
[9] A. Kirakosian, R. Bennewitz, F. J. Himpsel, and L. W. Bruch, Phys. Rev. B **67**, 205412 (2003).
[10] P. W. Anderson, Phys. Rev. **109**, 1492 (1958).
[11] H. W. Yeom *et al.*, Phys. Rev. B **72**, 035323 (2005).
[12] P. C. Snijders, S. Rogge, and H. H. Weitering, Phys. Rev. Lett. **96**, 076801 (2006).
[13] J. N. Crain, M. D. Stiles, J. A. Stroscio, and D. T. Pierce, Phys. Rev. Lett. **96**, 156801 (2006).
[14] A. Kirakosian *et al.*, Surf. Sci. **532**, 928 (2003).
[15] S. C. Erwin, Phys. Rev. Lett. **91**, 206101 (2003).
[16] H. S. Yoon, S. J. Park, J. E. Lee, C. N. Whang, and I. W. Lyo, Phys. Rev. Lett. **92**, 096801 (2004).
[17] W. H. Choi, P. G. Kang, K. D. Ryang, and H. W. Yeom, Phys. Rev. Lett. **100**, 126801 (2008).
[18] R. Bennewitz *et al.*, Nanotechnology **13**, 499 (2002).
[19] H. M. Zhang, T. Balasubramanian, and R. I. G. Uhrberg, Phys. Rev. B **65**, 035314 (2001).
[20] H. S. Yoon, J. E. Lee, S. J. Park, I. W. Lyo, and M. H. Kang, Phys. Rev. B **72**, 155443 (2005).
[21] S. Riikonen and D. Sánchez-Portal, Phys. Rev. B **71**, 235423 (2005); C.-Y. Ren, S.-F. Tsay, and F.-C. Chuang, *ibid.***76**, 075414 (2007).
[22] See EPAPS Document No. E-PRLTAO-100-010815 for a STM movie. This STM movie was measured over the inhomogeneous contrast (10 nm × 2 nm) shown in Fig. 1(b). STM imaging was performed at +1.0 V (an empty state) with a tunneling current of 50 pA and a scan speed of 1.6 s per frame. This clearly shows the dynamic fluctuation of the newly found inhomogeneity on the atomic wires of Si(111)-(5 × 2)-Au. For more information on EPAPS, see http://www.aip.org/pubservs/epaps.html.
[23] Y. Frenkel and T. Kontorova, J. Phys. (Moscow) **1**, 137 (1939).